

Biosynthesis of zinc oxide nanoparticles using *Albizia lebbek* stem bark, and evaluation of its antimicrobial, antioxidant, and cytotoxic activities on human breast cancer cell lines

This article was published in the following Dove Press journal:
International Journal of Nanomedicine

Huzaifa Umar¹⁻³
Doga Kavaz¹⁻³
Nahit Rizaner¹⁻³

¹Department of Bioengineering, Institute of Graduate Studies and Research, Cyprus International University, Mersin, Turkey;

²Biotechnology Research Center, Cyprus International University, Mersin, Turkey; ³Bioengineering Department, Cyprus International University, Mersin, Turkey

Background: Biocompatibility and stability of zinc oxide nanoparticles (ZnO NPs) synthesized using plants is an interesting research area of study in nanotechnology, due to its wide applications in biomedical, industrial, cell imaging, and biosensor fields. The present study reports the novel green synthesis of stable ZnO NPs using various concentrations of zinc nitrate (0.01M, 0.05M, 0.1M) and *Albizia lebbek* stem bark extracts as an efficient chelating agent. Antimicrobial, antioxidant, cytotoxic, and antiproliferative activities of the synthesized NPs on human breast cancer cell lines were evaluated using different assays.

Methods: Characterization of the synthesized ZnO NPs were carried out using various spectroscopic and microscopic techniques. Antimicrobial activity evaluation using disc diffusion method, antioxidant activity using hydrogen peroxide (H₂O₂) free radical scavenging assay and cytotoxic activity on MDA-MB 231 and MCF-7 using trypan blue dye exclusion and MTT assay.

Results: The UV-vis spectroscopy result revealed an absorption peak in the range of 370 nm. The involvements of *A. lebbek* bioactive compounds in the stabilization of the ZnO NPs were confirmed by X-ray diffraction and Fourier transform infrared analysis. Zeta sizer studies showed an average size of 66.25 nm with a polydispersity index of 0.262. Scanning electron microscopy (SEM) and energy-dispersive X-ray spectroscopy (EDX) analyses results revealed irregular spherical morphology and the presence of primarily Zn, C, O, Na, P, and K, respectively. The biosynthesized ZnO NPs revealed strong antimicrobial potentials against various gram-negative and gram-positive bacterial pathogens. Antioxidant activities carried out using H₂O₂ free radical scavenging assay revealed higher IC₅₀ values of 48.5, 48.7, and 60.2 µg/mL for 0.1M, 0.05M, and 0.01M ZnO NPs, respectively. Moreover, the biosynthesized ZnO NPs showed significant cytotoxic effects on MDA-MB 231 and MCF-7 breast cancer cell lines ($P < 0.001$, $n \geq 3$) in a concentration-dependent manner.

Conclusion: Overall, various concentrations of ZnO NPs were synthesized through a stable, simple, and eco-friendly green route via the use of *A. lebbek* stem bark extract. The biosynthesized ZnO NPs showed strong antimicrobial, antioxidant and cytotoxic activity against strongly and weakly metastatic breast cancer cell lines.

Keywords: biosynthesis, antimicrobial, antioxidant, cytotoxic, biocompatibility

Introduction

Nanotechnology is a rapidly growing area of studies that utilizes biosynthetic and environmental-friendly technology for the purpose of synthesis of zinc oxide nanoparticles (ZnO NPs), which are known to be nontoxic, chemically stable, biocompatible, and could be used as drug carriers,¹ cell imaging agents,² anticancer agents,³ antimicrobials,⁴ biosensors,⁵ antidiabetics,⁶ and cosmetics,⁷ because of their novel physicochemical

Correspondence: Huzaifa Umar
Department of Bioengineering, Institute of Graduate Studies and Research, Cyprus International University, 98258 Northern Cyprus via Mersin 10, Turkey
Tel +90 542 888 8419
Email humar@ciu.edu.tr

properties. Biocompatibility of zinc has been attributed to its presence in human system as the second most common and essential trace elements after iron with diverse role in body metabolic activities, and it is the fourth most commonly consumed metals worldwide.⁸ The physical and chemical methods that are used for the synthesis of metal oxide NPs are expensive and toxic, and antagonistic chemicals are used as a stabilizing agent.⁹ Metals oxide NPs modifications could be achieved by substitution with specific atoms, which then enhance optical, mechanical, and electrical properties of materials by changing their chemical surface properties.¹⁰ ZnO NPs have recently gained special attention due to their hexagonal phase, n-type semiconductor, and wurzite structure.¹¹ Green biosynthesis of ZnO NPs is simple, viable, and cost-effective and provides high yield with novel physical appearance, compared with other NPs such as silver, gold, titanium, and nickel.¹²

Recent studies have demonstrated the antibacterial potential of ZnO NPs through disruption of the cell membrane integrity, against extended-spectrum beta-lactamase-producing bacteria *Klebsiella pneumonia* and *Escherichia coli*.¹³ It has been recommended that ZnO NPs could retard *E. coli* growth through disorganizing the bacterial cell membrane, which increases permeability of the NPs through the membrane, leading to its accumulation in the cytoplasm and cell disruption.¹⁴ However, some microorganisms appear to show strong resistance against ZnO, but ZnO NPs showed strong antimicrobial activities on certain pathogenic bacteria such as *Salmonella enteritidis*, *Listeria monocytogenes*, *Bacillus subtilis*, *Staphylococcus aureus*, and *E. coli*.^{15–17} Medicinal plants are known to possess vitamins, terpenoids, and phenolic compounds that have antioxidant potentials,¹⁸ but literature showed that synthesized NPs using medicinal plants as dispersing agents display more antioxidant activity in vitro.¹⁹ Suresh et al reported ZnO NPs synthesized using *Cassia fistula* to exhibit significant antioxidant activities through scavenging of 1, 1-diphenyl-2-picrylhydrazil (DPPH) radicals.²⁰ Investigations on the cytotoxic activity of ZnO NPs demonstrate cytotoxic effect against cancerous cells and normal cells including lung epithelial cells²¹ and human lens epithelial cells.²² Green synthesis of ZnO NPs using various medicinal plants including *Costus pictus* D. Don,²³ *Pongamia pinnata*,²⁴ *Vitex negundo*,²⁵ and *Cassia auriculata*²⁶ has been reported to exhibit cytotoxic activity.

Albizia lebbbeck is a tropical species that belongs to *Albizia* genus, mostly growing to an average height of 24 m, trunk width of 50 cm, and seed pods that contain 6–12 seeds. The plant is widely distributed in Australia, Asia, Africa, and Southern America.²⁷ The seeds of the plant demonstrate anti-tumor, antifungal, and antibacterial activities against HepG2

hepatoma cells, fungi *Rhizoctonia solani*, and *E. coli*.²⁸ The leaves of the plant contain phytochemicals such as flavonoids, tannins, alkaloids, triterpenoid saponins, and cardiac glycosides that have therapeutic value.²⁹

In the present study, cost-effective green synthesis of ZnO NPs using *A. lebbbeck* aqueous extract as a capping agent and their characterization using various spectroscopic techniques are reported. The antibacterial activity of the synthesized NPs was studied against five pathogenic microorganisms: two gram-positive (*Bacillus cereus* and *S. aureus*) and three gram-negative (*E. coli*, *K. pneumoniae*, and *Salmonella typhi*). The in vitro free radical scavenging activity of ZnO NPs was assessed by hydrogen peroxide (H₂O₂) free radical scavenging assay. Furthermore, we investigated antiproliferative and cytotoxic activities of the NPs against human breast cancer lines MDA-MB 231 and MCF-7. The results are reported and images are presented.

Materials and methods

Preparation of *A. lebbbeck* extract

Fresh stem barks of *A. lebbbeck* were collected from Gaya Local Government Area, Kano State (Nigeria: 11° 52' 5" N and 9° 0' 40" E) and authenticated by a botanist at the herbarium of the Department of Plant Biology, Bayero University Kano, Nigeria. The specimen was given a voucher number BUKHAN187 and was deposited at the herbarium of the institute. The barks were washed properly with deionized water, shade dried, and then pulverized into coarse powder using mortar and pestle. *A. lebbbeck* aqueous extract was prepared by slight modifications of the method described by Suresh et al.²⁰ Briefly, the extraction was performed using water as a solvent in which 20 g of the coarse powder was soaked in 100 mL deionized water in a conical flask and was heated in a water bath under constant shaking at 45°C for 24 hours. The extract was then filtered using Whatman No 1 filter paper and the filtrate was stored at 4°C until used.

Synthesis of ZnO nanoparticles

ZnO NPs were prepared successfully using *A. lebbbeck* aqueous extract by the method of Elham Zare et al with slight modifications.³⁰ The ZnO NPs were synthesized using 0.01M, 0.05M, and 0.1M Zn(NO₃)₂·6H₂O solution in 90 mL distilled water; then, 10 mL of the prepared *A. lebbbeck* extract was added dropwise into the zinc nitrate solutions under constant stirring at 60°C for 5 hours to achieve a complex formation, and NaOH (5M) was added to the solution during stirring process to adjust the pH. Both the extract (control) and the mixture (zinc nitrate + extract) were then calcined at 350°C±10°C for 2 hours in a muffle furnace to obtain ZnO NPs.

Characterization

The synthesized ZnO NPs were characterized using various spectroscopic and microscopic techniques. UV–visible spectrum was evaluated using UV–Visible spectrophotometer (Shimadzu UV-2450) and the spectrum was recorded between 300 and 800 nm. Hydrodynamic (Z-average) size and polydispersity index (PDI) of the synthesized ZnO NPs were evaluated by Zeta sizer instrument (Malvern Zetasizer Nano ZS90), and the results were acquired by the Malvern ZS nano software. Fourier transform infrared (FTIR) analysis of the NPs was carried out with Fourier transform spectrometer (Shimadzu FT-IR Prestige-21 Model) at a frequency range of 4,000–500 cm^{-1} . Crystalline structure was analyzed using X-ray diffractometer (Rigaku ZSX Primus II). Morphological analysis of the synthesized ZnO NPs coated with platinum was carried out using scanning electron microscope (SEM) (JOEL JSM 6335-F) equipped with 150 kV acceleration voltage, and energy-dispersive X-ray spectroscopy (EDS) (Oxford Instruments AZTEC EDS) attached to the same instrument was used to ascertain the elemental composition and purity of the synthesized ZnO NPs.

Antimicrobial activity

Evaluation of antimicrobial activity of *A. lebeck* ZnO NPs against five pathogenic microorganisms – two gram-positive, *B. cereus* (ATCC 7064) and *S. aureus* (6538 P), and three gram-negative, *E. coli* (O157:H7), *K. pneumoniae* (ATCC 27738), and *S. typhi* (B-4420) – was carried out on Muller–Hilton agar dishes using disc diffusion method.³¹ Ciprofloxacin (10 $\mu\text{g}/\text{disc}$) was used as a standard and sterile blank disc with 5 mm diameter infused with known concentration of ZnO NPs, extracts, and dimethylsulfoxide (DMSO) was used to ascertain the antibacterial activity. Pure culture of the microorganisms was provided by the Department of Food Engineering Laboratory, Faculty of Engineering, Ege University, Turkey.

Antioxidant activity

Antioxidant activity was carried out by hydrogen peroxide (H_2O_2) free radical scavenging assay using the method of Pick and Mizel with some modifications.³² Briefly, various concentrations (100, 75, 50, 25, 12.5, and 6.25 $\mu\text{g}/\text{mL}$) of the synthesized ZnO NPs, extract, and ascorbic acid as standard, were mixed with 100 μL H_2O_2 solution (5 mM), and the absorbance was read at 230 nm after 20 minutes of incubation. PBS without hydrogen peroxide was used as a blank solution. The percentage inhibition of H_2O_2 scavenging was calculated using the following equation:

$$\% \text{H}_2\text{O}_2 \text{ free radicals} = \left[1 - \left(\frac{A_s}{A_c} \right) \right] \times 100$$

where A_c is the absorbance of control and A_s is the absorbance of sample.

Cell culture

Breast cancer cell lines MDA-MB 231 and MCF-7 were obtained from Professor Dr Mustafa Djamgoz (Imperial College London, UK), and the use of the cell lines was approved by Biotechnology Research Center Ethical Committee (BRCEC2011-01). Cells were cultured in DMEM (Gibco by Life Technology, Carlsbad, CA) supplemented with 10% 2 mM L-glutamine, and penicillin/streptomycin. The cells were constantly maintained under cell culture conditions of 37°C and 5% CO_2 in a humidified chamber. All the chemicals used for the cell culture are of analytical grades.

Cytotoxicity and proliferation assay

Cytotoxic activity of the ZnO NPs was evaluated by trypan blue dye exclusion assay on breast cancer cell lines MDA-MB 231 and MCF-7.³³ The assay was performed to determine whether the ZnO NPs have toxic effect on the cell lines. The cells were plated in 35 mm dishes, incubated overnight, and treated with various concentrations (100, 50, 25, and 5 $\mu\text{g}/\text{mL}$) of the synthesized ZnO NPs. After the treatment, trypan blue dye (4%) was added into the 35 mm cell culture dishes and incubated for 10 minutes. Thirty random fields of view with at least 20 cells in each field were viewed at 100 \times using an inverted microscope (Leica DFC295) and the number of live vs dead cells was determined.

Antiproliferative activity of the synthesized ZnO NPs was analyzed using MTT reagent (Sigma-Aldrich) as previously described by Fraser et al with slight modifications.³⁴ Briefly, cells (MDA-MB 231 and MCF-7) were plated in 12-well Falcon tissue plates at a density of 3×10^4 cells/well in 1 mL DMEM and allowed to settle overnight. After that, the DMEM was removed and replaced with various concentrations of ZnO NPs viz., 5, 25, 50, and 100 $\mu\text{g}/\text{mL}$ (minimum three wells per each concentration), and then incubated for 24 hours. After the treatment periods, the medium was removed, and 0.15 mL MTT was added to 0.6 mL fresh medium. The plates were then wrapped in foil and incubated at 37°C for 3 hours. The medium containing the MTT was substituted with 0.89 mL DMSO and 0.11 mL glycine buffer. Absorbance was measured using Absorbance Microplate Reader (ELX 800™) at a wavelength of 570 nm after 10 minutes.

Statistical analysis

Data are given as means \pm standard errors of the mean (SEM). Graphical representations and statistical analysis were done using OriginPro (version 2016) and InStatGraphPad software (version 3). Statistical comparisons were determined using one-way ANOVA followed by Tukey–Kramer multiple comparison test, where necessary. All the experiments were carried out in triplicate and repeated at least three times ($n \geq 3$). $P < 0.05$ was considered significant or $P > 0.05$ insignificant and $P < 0.0001$ was considered highly significant.

Results and discussion

In this present study, ZnO NPs were rapidly synthesized using *A. lebbeck* stem bark extract as bioreductant.

UV–vis spectroscopy was employed to analyze the formation of ZnO NPs from zinc nitrate solution, since there is a visible color change (from dark brown to light brown) that occurred, which indicates the formation of ZnO NPs (Figure 1). Intensity of the light brown color of the NPs increased with increase in the concentration of zinc nitrate, which could be due to the excitation of surface plasmon vibrations.³⁵

UV–visible absorption of the synthesized ZnO NPs with various concentrations of zinc nitrate and pH at different incubation periods are shown in Figure 2A and B. The results of our study show that the absorption peak for the synthesized ZnO NPs is 368 nm, and is in conformity with the range of light absorption of ZnO NPs, which is 360–380 nm.³⁶ Elham Zare et al reported the biosynthesis of ZnO NPs using cumin seeds and zinc nitrate, with an average size of 7 nm and UV–vis absorption peak at 370 nm.³⁰ Additionally, Singh et al also reported the green synthesis of ZnO NPs using *Pseudomonas aeruginosa* and zinc nitrate, with a size between 35 and 80 nm and UV–vis absorption at 360 nm.³⁷ Also, some physico-chemical parameters such as concentration of metal ions, pH, and incubation period were studied to determine the suitable condition for the synthesis of ZnO NPs (Figure 2A and B).

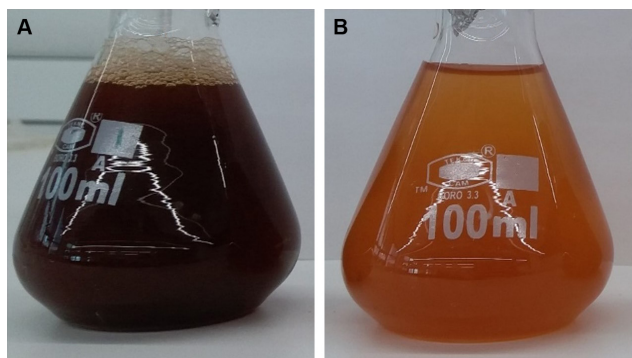


Figure 1 Synthesis of ZnO NPs: (A) *Albizia lebbeck* aqueous extract; (B) ZnO NPs. **Abbreviation:** ZnO NPs, zinc oxide nanoparticles.

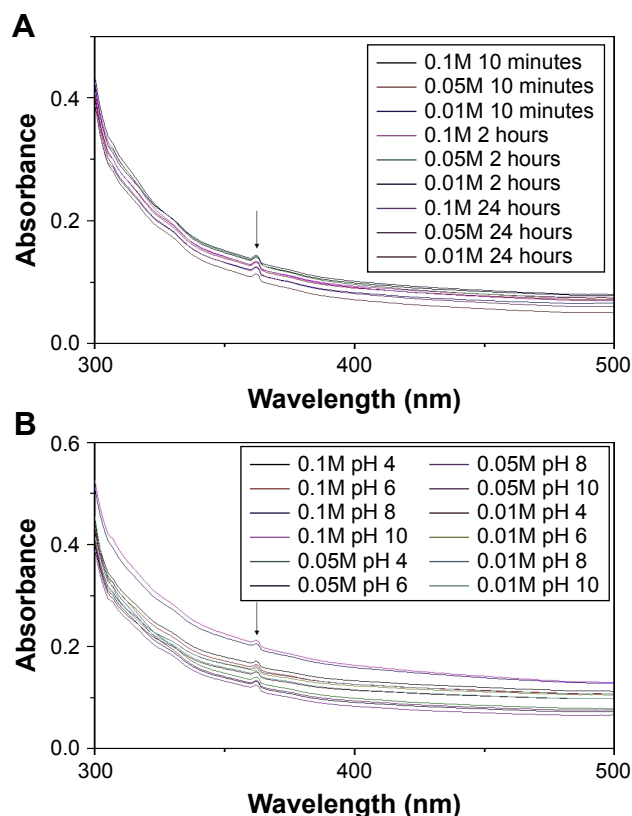


Figure 2 UV–visible spectra of ZnO NPs prepared with various concentrations of zinc nitrate at different (A) incubation time and (B) pH.

Abbreviation: ZnO NPs, zinc oxide nanoparticles.

Increasing the concentrations of the metal ions (zinc nitrate) from 0.01 to 0.1M did not directly show any significant effect on the absorption peak but it revealed effect on the intensity of the synthesized ZnO NPs with increased metal ion concentrations. The pH was regulated using 0.1M NaOH and 0.1 HCl. At pH 4, 6, and 8, the nanoparticle was synthesized but there was a slight shift in the absorption intensity of the synthesized ZnO NPs; however, at pH 10, no effect on both the intensity and the absorption peak of the nanoparticle was observed. Nagarajan et al revealed that, at lower pH 4–5 and higher pH 10, ZnO NPs synthesized using seaweed did not show absorption.³⁶ The presence of absorption peaks at those pH in our study could be a result of high carboxylic acid content present in *A. lebbeck* stem bark extract.²⁹ Similarly, measuring the UV–vis spectra of the synthesized ZnO NPs at different time intervals after the synthesis did not show any effect on the absorption peak and intensity (Figure 2A), and it reflects the stability of the synthesized ZnO NPs as suspension after 24 hours.

Hydrodynamic size distribution results of the ZnO NPs were obtained by the dynamic light scattering analysis of the particles to confirm the synthesis of the NPs; the Z-average size of the 0.05M and 0.1M ZnO NPs was 82.31 nm and average PDI was 0.262 (Figure 3A and B). The Z-average of 0.01M

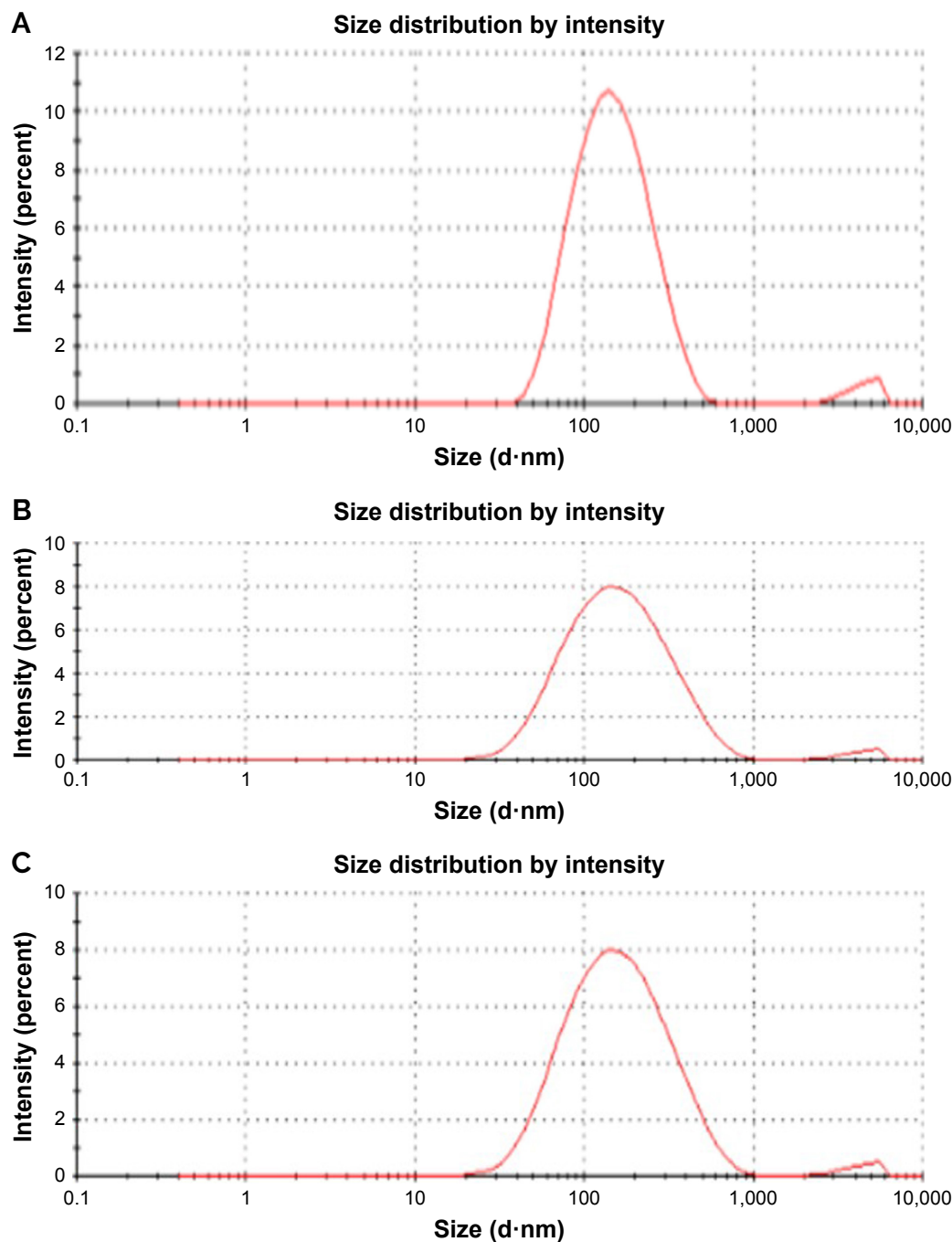


Figure 3 Particle size distribution of synthesized ZnO NPs using *Albizia lebbek* stem bark extract: (A) 0.1M, (B) 0.05M, and (C) 0.01M. **Abbreviation:** ZnO NPs, zinc oxide nanoparticles.

synthesized NPs was 110 nm, and PDI was 0.326 (Figure 3C). Our zeta sizer results clearly reveal that the synthesized ZnO NPs are monodispersed in nature due to their broad size distribution and show PDI values of <0.7 , and this confirmed the monodispersity of ZnO NPs.³⁸ Particle size can be elucidated more with transmission electron microscope or SEM.³⁹ The result obtained was almost similar to our SEM data.

FTIR analysis of the synthesized ZnO NPs was carried out at room temperature and a frequency range between 400

and $4,500\text{ cm}^{-1}$. The FTIR spectra show the composition of the bioactive molecules of *A. lebbek* and their distribution on the surface of the ZnO NPs. Synthesized ZnO NPs and *A. lebbek* spectra, shown in Figure 4, revealed the different absorption bands of the NPs and the plant extract, respectively. Wide absorption bands around $3,356\text{ cm}^{-1}$ were associated with O–H bending of the water molecules, which were adsorbed on the sample.⁴⁰ FTIR spectrum of the ZnO NPs (0.01M, 0.05M, and 0.1M) prepared with

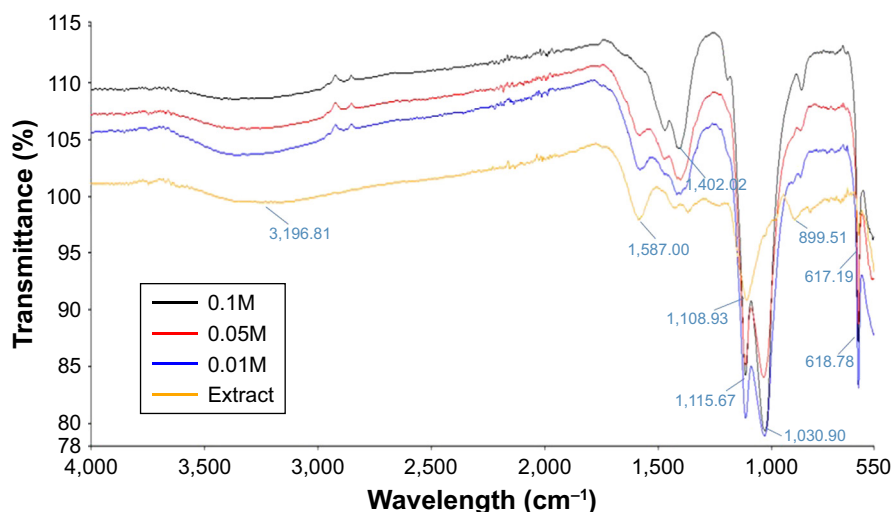


Figure 4 FTIR spectra of *Albizia lebbek* extract and synthesized ZnO NPs using various concentrations of zinc nitrate.
Abbreviations: FTIR, Fourier transform infrared; ZnO NPs, zinc oxide nanoparticles.

the *A. lebbek* extract absorbed at 1,402, 1,115, 1,030, and 618 cm^{-1} . The absorption peak at 1,402 cm^{-1} correspond to C=CH stretching of methyl group, and 1,030 cm^{-1} implies the presence of C=O amide band of aliphatic carboxylic acid. The absorption peak observed at 1,030 cm^{-1} can be attributed to C–O of primary saturated alcohol. The bands observed at 618 cm^{-1} correspond to Zn–O bond, which confirms that the synthesized nanoparticle is a ZnO NP.⁴¹ Our FTIR analysis revealed that carboxylic acid and alcoholic compounds are

capable of binding metals, and may form metal NPs through stabilizing the medium and preventing agglomeration.²³

Phase purity of the various concentrations of the biosynthesized ZnO NPs using *A. lebbek* extract was studied using X-ray diffraction (XRD). Figure 5 shows the XRD spectrum of the biosynthesized ZnO NPs. The main peaks obtained at 100, 002, 101, 102, 110, 103, 112, 004, and 104 correspond to Bragg reflections with 2θ values of 31.70°, 34.34°, 36.16°, 47.54°, 56.48°, 62.78°, 67.66°, 72.53°, and 76.58°

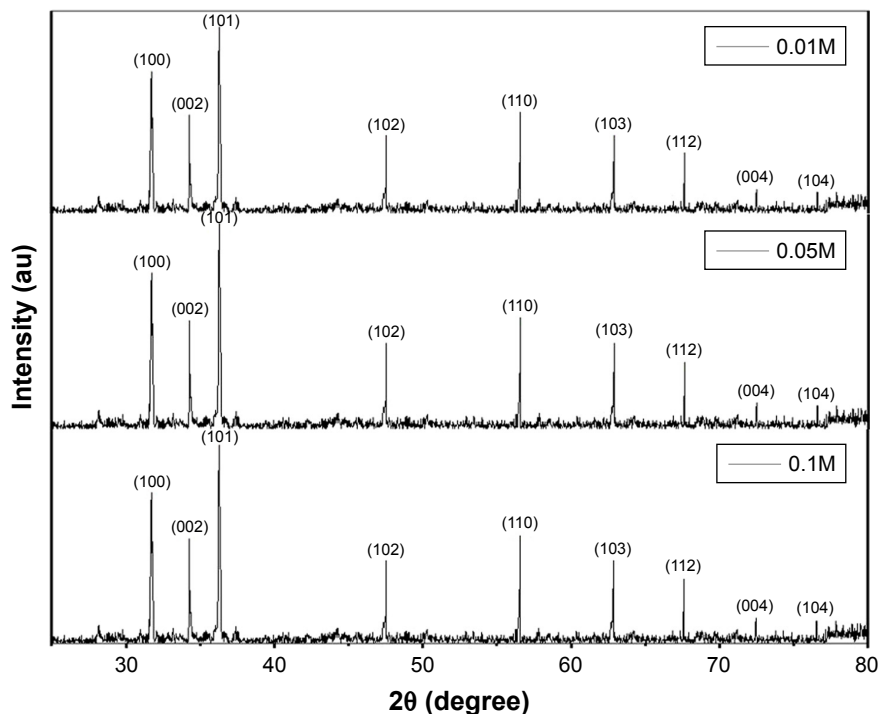


Figure 5 XRD pattern of 0.01M, 0.05M, and 0.1M synthesized ZnO NPs.
Abbreviations: XRD, X-ray diffraction; ZnO NPs, zinc oxide nanoparticles.

respectively. The presence of the peaks confirms the formation of highly purified ZnO NPs. Synthesized ZnO NPs using various concentrations of 0.01M, 0.05M, and 0.1M reveal similar XRD spectrum pattern. The XRD spectrum obtained indicates the absence of impurities. Furthermore, the pattern shows that the ZnO NPs were synthesized using natural source.³⁰

The surface morphology of synthesized ZnO NPs was explored using SEM. Typical SEM micrographs display many agglomerated particles with irregular spherical morphology, and the various concentrations of 0.1M, 0.05M, and 0.01M ZnO NPs reveal average diameter sizes of 66.25, 82.52, and 112.87 nm, respectively (Figure 6A–C). The ZnO NPs appear to be more agglomerated, and some of the crystals are more visible in Figure 6A. In Figure 6B, the particles

reveal slight agglomeration of zinc oxides and appear to be elongated and hexagonal shaped, and some particles in Figure 6C appear to be elongated and rod-like shaped. Raut et al synthesized ZnO NPs using *Ocimum tenuiflorum* extract, which revealed hexagonal and rod-shaped NPs with size ranging between 11 and 25 nm.⁴²

Energy-dispersive X-ray (EDX) spectra revealed the surface chemical composition of the synthesized ZnO NPs. Three clear signals of Zn and one signal of C, O, Na, P, and K were observed in both particles, but there is a presence of an additional signal of S in 0.05M and two signals of Mg and Cl in 0.01 ZnO NPs (Figure 6D–F). The presence of small signals of C, O, P, K, S, Mg, and Cl in the EDX spectrum confirmed the presence of the bioactive compounds of

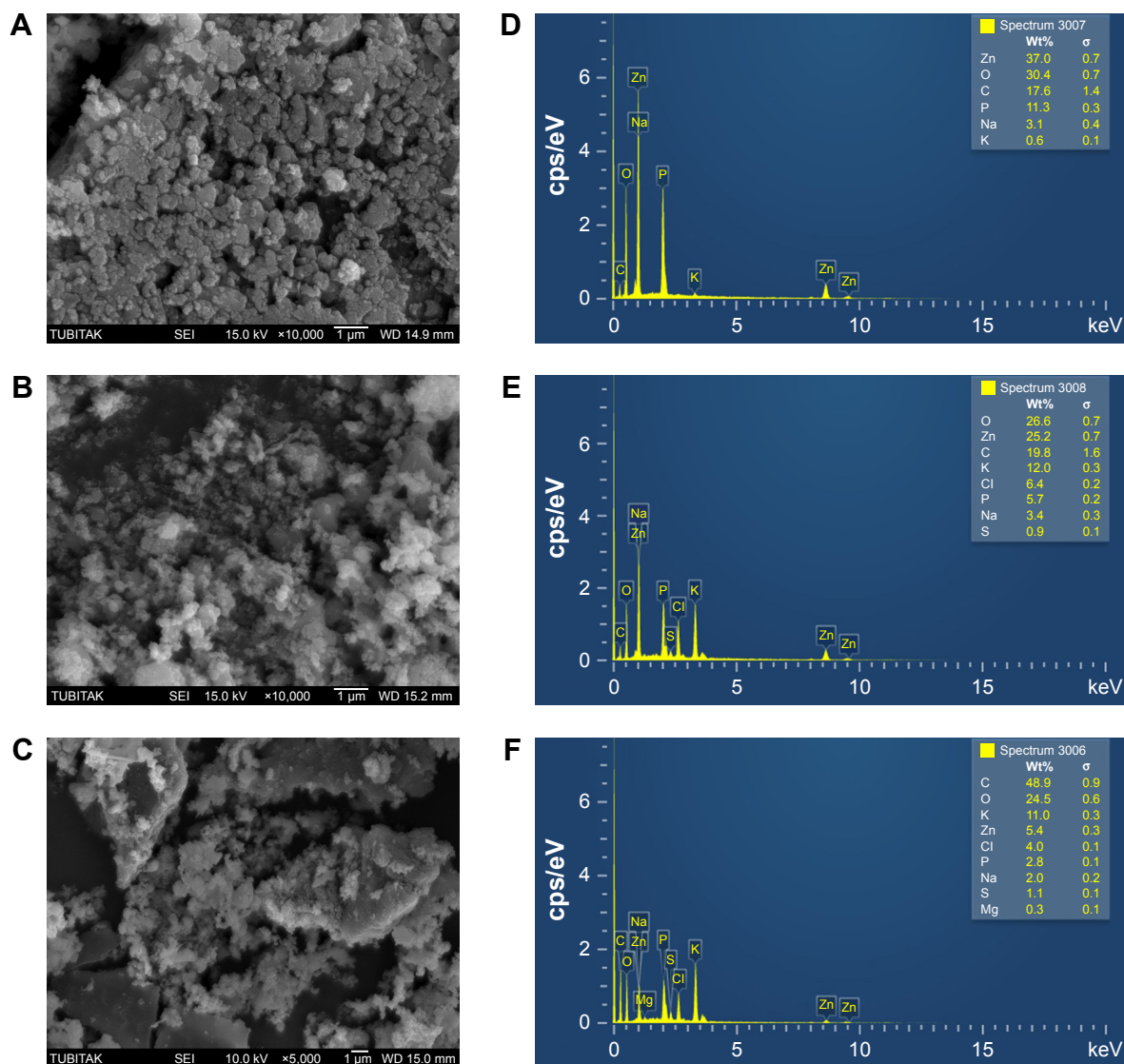


Figure 6 SEM images of ZnO NPs synthesized using *Albizia lebeck* stem bark extract: (A) 0.1M, (B) 0.05M, and (C) 0.01M. EDX spectra of the ZnO NPs: (D) 0.1M, (E) 0.05M, and (F) 0.01M.

Abbreviations: EDX, energy-dispersive X-ray spectroscopy; SEM, scanning electron microscope; ZnO NPs, zinc oxide nanoparticles; cps/eV, counts per second per electron-volt.

Table 1 Antimicrobial activity of ZnO NPs in comparison with extract, zinc nitrate solution, DMSO, and antibiotics

Bacterial strains	<i>Bacillus cereus</i> (mean ± SEM)	<i>Staphylococcus aureus</i> (mean ± SEM)	<i>Escherichia coli</i> (mean ± SEM)	<i>Klebsiella pneumoniae</i> (mean ± SEM)	<i>Salmonella typhi</i> (mean ± SEM)
Standard ciprofloxacin (10 µg/disc)	10.7±0.56	10.3±0.56	14.0±0.20	11.0±0.30	12.53±0.50
ZnO NPs (0.1M)	8.83±0.42	4.50±0.30**	9.13±0.41**	7.30±0.29**	10.57±0.320
ZnO NPs (0.05M)	5.5±0.50**	5.67±0.29**	7.67±0.47**	3.33±0.28**	6.5±0.20**
ZnO NPs (0.01M)	3.33±0.29**	2.00±0.22**	4.67±0.15**	3.67±0.21**	1.00±0.10**
<i>Albizia lebbek</i> extract	1.0±0.20**	1.5±0.20**	0.3±0.15**	1.0±0.10**	0.97±0.31**
Zinc nitrate solution (0.1M)	2.67±0.15**	2.33±0.29**	1.0±0.10**	1.33±0.21**	1.0±0.20**
DMSO (30%)	–	–	–	–	–

Notes: Results are presented as mean ± SEM of inhibition zone (mm) of at least triplicates (n≥3). **P<0.01 vs control (standard group). (–) indicates no significant antibacterial activity.

Abbreviations: DMSO, dimethylsulfoxide; SEM, standard error of mean; ZnO NPs, zinc oxide nanoparticles.

A. lebbek stem bark on the surface of the synthesized ZnO NPs, and the Na signal in both particles could as a result of pH regulation during the synthesis of the NPs. Elemental mapping analysis of the synthesized ZnO NPs revealed 37% distribution of zinc in 0.1M, 25.2% in 0.05M, and 5.4% in 0.01M. The EDS results revealed the highest proportion of zinc in 0.1M and 0.05M, and could ascertain the green synthesis of ZnO NPs. Additionally, the optical absorption signals of zinc shown by the synthesized ZnO NPs were due to plasmon resonance of ZnO NPs.³⁶

Antimicrobial activity

The results of the antimicrobial activities of the synthesized ZnO NPs, extract, zinc nitrate solution, DMSO, and antibiotics evaluated using agar disc diffusion method against five pathogenic bacterial strains are shown in Table 1.

While analyzing the antimicrobial activities of the synthesized ZnO NPs, we observed that the inhibitory effects of 0.1M ZnO NPs against *B. cereus* and *S. typhi* revealed no significant difference when compared with those of ciprofloxacin (standard), and significant differences were observed against *S. aureus*, *E. coli*, and *K. pneumoniae* (Table 1 and Figure 7). The lower concentrations of ZnO

NPs demonstrated moderate inhibitory effect against both gram-negative and gram-positive bacteria tested. The *A. lebbek* aqueous extract showed mild activity, and zinc nitrate solution revealed moderate to mild activity against all the bacterial strains tested. DMSO used a solvent did not demonstrate any antibacterial activity (Table 1).

The results revealed that gram-negative bacteria are less resistant to ZnO NPs treatments than gram-positive bacteria, and this could attributed to the presence of a thick layer in the cell walls (peptidoglycan) of the latter group. Sinha et al studied the effect of ZnO NPs on halophilic and mesophilic bacterial species and revealed that *Enterobacteria*, which is gram-negative, is more sensitive to these NPs than *B. subtilis*, which is gram-positive bacteria; They concluded that the resistance in gram-positive bacteria is due to the presence of a thick layer of peptidoglycan in their cell wall.⁴³ Elham Zare et al also found a strong antibacterial potential against gram-negative bacteria using ZnO NPs synthesized from cumin seeds, and concluded that the slight resistance of gram-positive bacteria is due the presence of a thick layer of peptidoglycan in their cell wall,³⁰ which is similar to the results achieved in this study. It has been reported that binding of zinc ion to the bacterial cell membrane and



Figure 7 Zone of inhibition of 0.1M synthesized ZnO NPs compared with extract, zinc nitrate solution, DMSO, and antibiotics: (a) extract, (b) zinc nitrate solution, (c) ZnO NPs, (d) DMSO, and (e) antibiotic (ciprofloxacin).

Abbreviations: DMSO, dimethylsulfoxide; ZnO NPs, zinc oxide nanoparticles.

production of reactive oxygen species (ROS) inside the cell result in the disruption of the cell.³⁰

Antioxidant activity

Antioxidant activity of the nanoparticles was studied using H₂O₂ free radical scavenging assay.

The results of the antioxidant activities of the ZnO NPs analyzed spectrophotometrically using H₂O₂ free radical scavenging assay are shown in Figure 8. The H₂O₂ activity of ascorbic acid, 0.1M ZnO NPs, 0.05M ZnO NPs, 0.01M ZnO NPs, and extract revealed IC₅₀ values of 45.7, 48.5, 48.7, 60.2, and 66.6 µg/mL, respectively. Additionally, 0.1M ZnO NPs

revealed the highest percentage inhibition among the NPs, followed by 0.05M ZnO NPs. The percentage inhibition shown by 0.1M ZnO NPs is close to that of ascorbic acid (standard), which could be due to increase in zinc ion concentration. The synthesized ZnO NPs revealed a concentration-dependent effect in H₂O₂ free radical scavenging activity. The extract revealed the lowest antioxidant activity as shown in Figure 8A. Increase in the antioxidant activity of the biosynthesized ZnO NPs when compared with the plant might be a result of metal ions present in the particles; the possible predicted mechanism is illustrated in Figure 8B. It has been reported that enzymes utilizing metal ion (Zn) as a cofactor scavenge H₂O₂ free

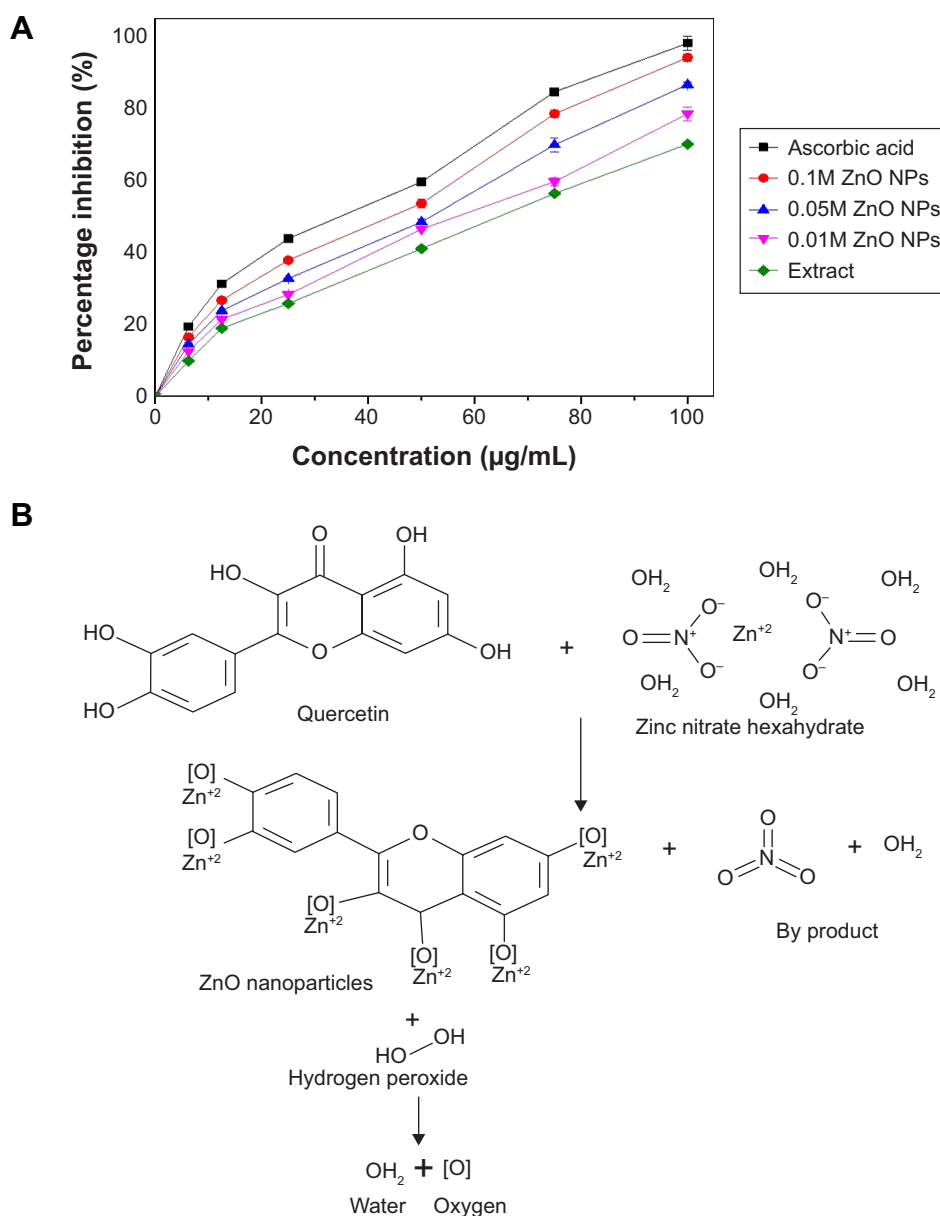


Figure 8 H₂O₂ free radical scavenging activity of the biosynthesized ZnO NPs.

Notes: (A) H₂O₂ free radical scavenging activity of the biosynthesized ZnO NPs. (B) Predicted mechanism of ZnO NPs formation and its H₂O₂ free radical scavenging activity.

Abbreviation: ZnO NPs, zinc oxide nanoparticles.

radicals, and the presence of Zn ion in particles might be responsible for higher H₂O₂ free radical scavenging activity when compared with the plant.⁴⁴ Parashant et al revealed that phenolic compounds present in plant extracts always demonstrated high antioxidant activity and they play an important role in the green synthesis of nanoparticles.⁴⁵

In vitro cytotoxic and antiproliferative activity

ZnO NPs were screened for cytotoxic activity against strongly metastatic and weakly metastatic breast cancer

(BCa) cell lines, MDA-MB 231 and MCF-7 cells, respectively. Trypan blue exclusion assay was carried out to ascertain the effects of different concentrations (5, 25, 50, and 100 µg/mL) of 0.1M, 0.05M, and 0.01M ZnO NPs on the viability of MDA-MB 231 and MCF-7 cells after 24-hour incubation period. The results showed that synthesized ZnO NPs significantly inhibited the viability of MDA-MB 231 cells with increased concentration when compared with control ($P < 0.001$, $n \geq 3$, Figure 9A). Typical phase-contrast light-microscopy images of ZnO NPs-treated MDA-MB 231 cells and controls obtained from trypan blue assays are

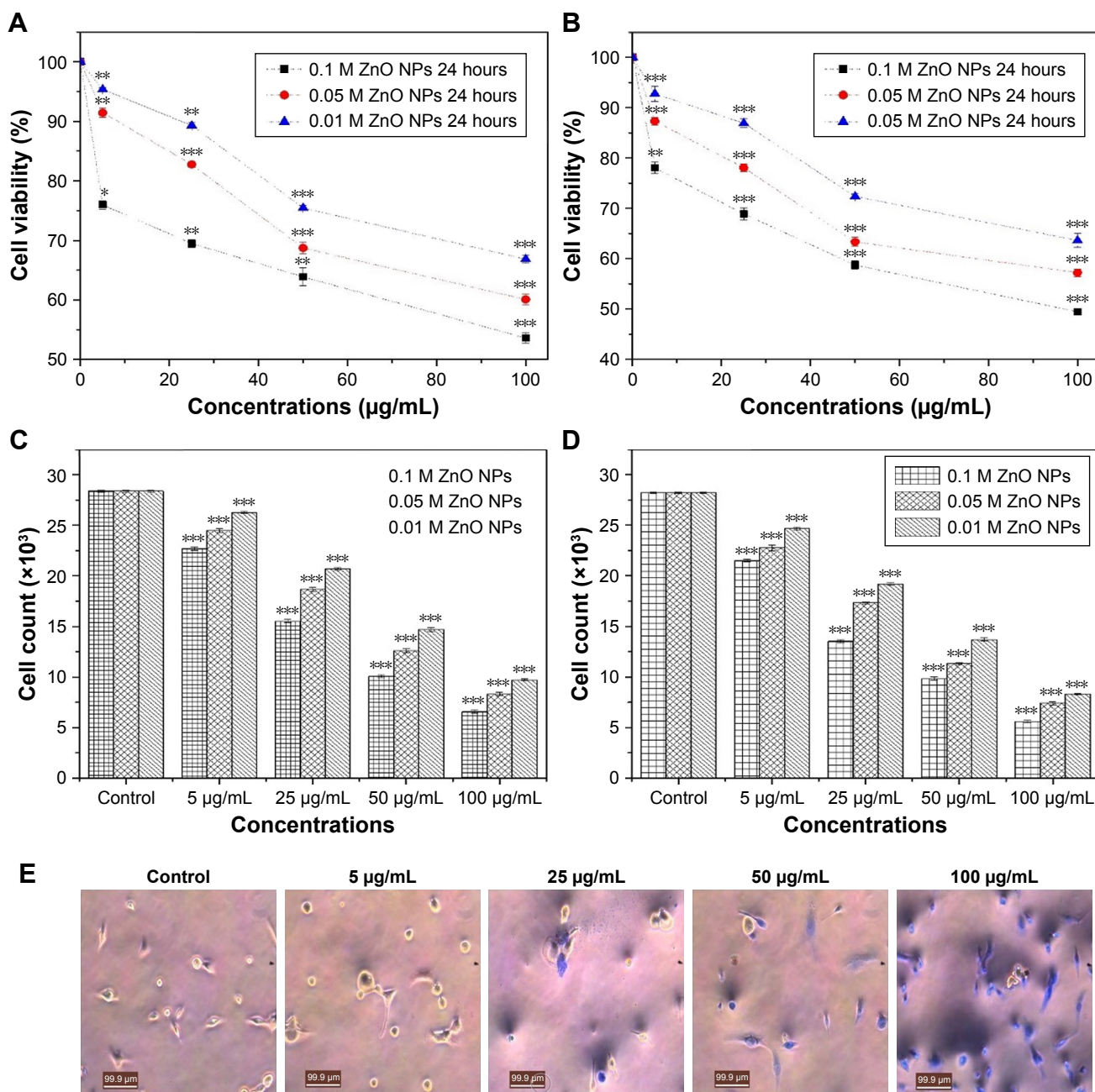


Figure 9 (Continued)

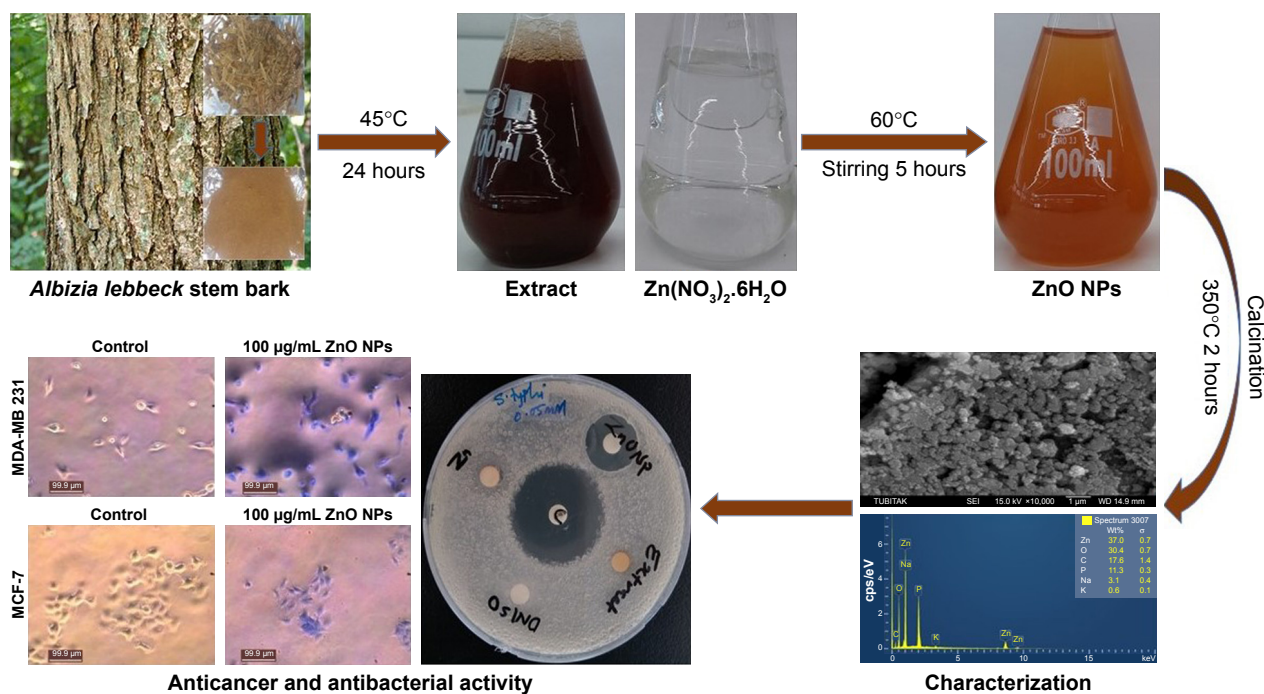


Figure 10 Summary of the synthesis and biomedical activity of biosynthesized ZnO NPs.

higher cytotoxic effects than 0.05M and 0.01M, which might be due to higher percentage of zinc in the nanoparticles. The 5 µg/mL dose of 0.05M and 0.01M synthesized ZnO NPs showed extremely significant difference when compared with control ($P < 0.001$, $n \geq 3$, Figure 9B), but a similar concentration of 0.1M ZnO NPs revealed significant difference upon comparison with the control ($P < 0.001$, $n \geq 3$, Figure 9A). Additionally, all the concentrations of ZnO NPs used in our study showed significant activity against MCF-7 cells when compared with control ($P < 0.5$, $n \geq 3$, Figure 9A and B). Typical phase-contrast light-microscopy images of ZnO NPs-treated MCF-7 cells and controls obtained from trypan blue assays are shown in Figure 9F. ZnO NPs showed a cytotoxic effect against colon cancer cell lines HT29, and the effect was found to increase with increased particle concentration.⁴⁶ Prashant et al reported the cytotoxic effect of ZnO nanopowders synthesized using *Punica granatum* and *Tamarindus indica* L. by combustion-assisted facile process against MCF-7 Bca cell line; the cytotoxic effects were found to be concentration dependent,⁴⁵ and the results were similar to those obtained in our studies.

The study also revealed effect on cell number as a confirmation of the cytotoxic effect of synthesized ZnO NPs on MDA-MB 231 and MCF-7 human Bca cell lines. Synthesized ZnO NPs of 0.1M, 0.05M, and 0.01M showed a significant decrease in the proliferation of both cell lines when compared with control ($P < 0.001$, $n \geq 3$, Figure 9C and D). The effects of

the NPs on cell number following 24 hours incubation period were also found to be concentration dependent. High reduction in the cell number of both cell lines was observed with 0.1M ZnO NPs in a concentration-dependent manner and 100 µg/mL inhibit the cell number of MDA-MB 231 and MCF-7 with 76.8% and 80.2%, respectively; this finding served as a confirmation for the cytotoxic effect as determined by trypan blue assay. Metal ion NPs and their peptide conjugates inhibit endothelial cell angiogenesis and proliferation through binding to endothelial growth factor, mitogens, and mediators of angiogenesis.³²

Membrane blebs were also observed on MDA-MB 231 and MCF-7 cells treated with ZnO NPs synthesized using *A. lebeck* stem bark, following 48 hours of incubation (Figure 9G and H). This may possibly indicate an alternative apoptotic mechanism experienced by MDA-MB 231 and MCF-7 cells as membrane blebs were observed in the cells upon exposure to ZnO NPs (Figure 9I). It has been reported that plasma membrane blebs are among the basic sign that indicate apoptosis in cells.⁴⁷ The plasma membrane blebs in our studies were also found to occur in a concentration-dependent manner as membrane blebs were not observed with the untreated cells (control) but were observed with treated cells in a concentration-dependent manner. Membrane blebbing and a decrease in cell viability observed in both cells might be a result of ROS, metal ions (Zn^{+2}), and other molecules released in the culture medium by the synthesized ZnO NPs.⁴⁸

Hanley et al revealed that the increase in intracellular level of Zn²⁺ ions and other molecules released from ZnO NPs are correlated with an increase in ROS generation, and this will lead to apoptosis.⁴⁹ The summary of the whole process involved can be seen in Figure 10.

Conclusion

Overall, various concentrations of ZnO NPs were synthesized through a stable, simple, and eco-friendly green route via the use of *A. lebeck* stem bark extract. The extract acts as both reducing and stabilizing agent, which was confirmed by FTIR analysis. The successful synthesis of 0.1M, 0.05M, and 0.01M ZnO NPs was confirmed by Zeta sizer, UV-vis, FTIR, XRD, SEM, and EDX analyses. The UV-vis spectroscopy revealed an absorption peak in the range of 370 nm. SEM results revealed many agglomerated particles with irregular hexagonal morphology and an average size of 66.25 nm. XRD spectrum revealed that the synthesized ZnO NPs have hexagonal wurzite structure. The biosynthesized ZnO NPs showed strong antimicrobial activity against *B. cereus*, *S. aureus*, *E. coli*, *K. pneumoniae*, and *S. typhi*. Various concentrations of the ZnO NPs demonstrated antioxidant activity. Additionally, the ZnO NPs showed significant cytotoxic effects and induction of membrane blebs on MDA-MB 231 and MCF-7 breast cancer cell lines in a concentration-dependent manner. The 0.1M ZnO NPs revealed the best biological activity compared with 0.05M and 0.01M nanoparticles and the whole process is illustrated in Figure 10.

Acknowledgments

The authors acknowledge the support of Prof. Dr. Mustapha Djamgoz, Department of Life Sciences, Faculty of Natural Sciences, Imperial College London.

Disclosure

The authors report no conflicts of interest in this work.

References

- Albrecht MA, Evans CW, Raston CL. Green chemistry and the health implications of nanoparticles. *Green Chem.* 2006;8(5):417–432.
- Xu D, Liu M, Zou H, et al. A new strategy for fabrication of water dispersible and biodegradable fluorescent organic nanoparticles with AIE and ESIP characteristics and their utilization for bioimaging. *Talanta.* 2017;174:803–808.
- Hassan HF, Mansour AM, Abo-Youssef AM, Elsadek BE, Messiha BA. Zinc oxide nanoparticles as a novel anticancer approach; in vitro and in vivo evidence. *Clin Exp Pharmacol Physiol.* 2017;44(2):235–243.
- Nirmala M, Anukaliani A. Synthesis and characterization of undoped and TM (Co, Mn) doped ZnO nanoparticles. *Mater Lett.* 2011;65(17–18):2645–2648.
- Thapa A, Soares AC, Soares JC, et al. Carbon nanotube matrix for highly sensitive biosensors to detect pancreatic cancer biomarker CA19-9. *ACS Appl Mater Interfaces.* 2017;9(31):25878–25886.
- El-Gharbawy RM, Emara AM, Abu-Risha SE. Zinc oxide nanoparticles and a standard antidiabetic drug restore the function and structure of beta cells in Type-2 diabetes. *Biomed Pharmacother.* 2016;84:810–820.
- Rosi NL, Mirkin CA. Nanostructures in biodiagnostics. *Chem Rev.* 2005;105(4):1547–1562.
- Jansen J, Karges W, Rink L. Zinc and diabetes – clinical links and molecular mechanisms. *J Nutr Biochem.* 2009;20(6):399–417.
- Li H, Carter JD, Labean TH. Nanofabrication by DNA self-assembly. *Mater Today.* 2009;12(5):24–32.
- Altıntaş YO, Unalan HE, Durucan C. Highly efficient room temperature synthesis of silver-doped zinc oxide (ZnO:Ag) nanoparticles: structural, optical, and photocatalytic properties. *J Am Ceram Soc.* 2013;96(3):766–773.
- Chauhan R, Kumar A, Chaudhary RP. Structures and optical properties of Zn_{1-x}NiO_x nanoparticles by co-precipitation method. *Res Chem Intermed.* 2012;38(7):1483–1493.
- Vigneshwaran N, Kumar S, Kathe AA, Varadarajan PV, Prasad V. Functional finishing of cotton fabrics using zinc oxide-soluble starch nanocomposites. *Nanotechnology.* 2006;17(20):S087–S095.
- Hameed ASH, Chandrasekaran K, Abdulazees PA. In vitro antibacterial activity of ZnO and Nd doped ZnO nanoparticles against ESBL producing *Escherichia coli* and *Klebsiella pneumoniae*. *Sci Rep.* 2016;6:24312.
- Brayner R, Ferrari-Illiou R, Brivois N, Djediat S, Benedetti MF, Fievet F. Toxicological impact studies based on *Escherichia coli* bacteria in ultrafine ZnO nanoparticles colloidal medium. *Nano Lett.* 2006;6(4):866–870.
- Adams LK, Lyon DY, Alvarez PJ. Comparative eco-toxicity of nano-scale TiO₂, SiO₂, and ZnO water suspensions. *Water Res.* 2006;40(19):3527–3532.
- Huang Z, Zheng X, Yan D, et al. Toxicological effect of ZnO nanoparticles based on bacteria. *Langmuir.* 2008;24(8):4140–4144.
- Jones N, Ray B, Ranjit KT, Manna AC. Antibacterial activity of ZnO nanoparticle suspensions on a broad spectrum of microorganisms. *FEMS Microbiol Lett.* 2008;279(1):71–76.
- Koleva II, van Beek TA, Linssen JP, de Groot A, Evstatieva LN. Screening of plant extracts for antioxidant activity: a comparative study on three testing methods. *Phytochem Anal.* 2002;13(1):8–17.
- Balan K, Qing W, Wang Y, et al. Antidiabetic activity of silver nanoparticles from green synthesis using *Lonicera japonica* leaf extract. *RSC Adv.* 2016;6(46):40162–40168.
- Suresh D, Nethravathi PC, Udayabhanu CG, Rajanaika H, Nagabhushana H, Sharma SC. Green synthesis of multifunctional zinc oxide (ZnO) nanoparticles using *Cassia fistula* plant extract and their photodegradative, antioxidant and antibacterial activities. *Mater Sci Semicond Process.* 2015;31:446–454.
- Zhang J, Qin X, Wang B, et al. Zinc oxide nanoparticles harness autophagy to induce cell death in lung epithelial cells. *Cell Death Dis.* 2017;8(7):e2954.
- Wang D, Guo D, Bi H, Wu Q, Tian Q, Du Y. Zinc oxide nanoparticles inhibit Ca²⁺-ATPase expression in human lens epithelial cells under UVB irradiation. *Toxicol In Vitro.* 2013;27(8):2117–2126.
- Suresh J, Pradheesh G, Alexramani V, Sundrarajan M, Hong SI. Green synthesis and characterization of zinc oxide nanoparticle using insulin plant (*Costus pictus* D. Don) and investigation of its antimicrobial as well as anticancer activities. *Adv Nat Sci Nanosci Nanotechnol.* 2018;9(1):015008.
- Sundrarajan M, Ambika S, Bharathi K. Plant-extract mediated synthesis of ZnO nanoparticles using *Pongamia pinnata* and their activity against pathogenic bacteria. *Adv Powder Technol.* 2015;26(5):1294–1299.
- Ambika S, Sundrarajan M. Antibacterial behaviour of *Vitex negundo* extract assisted ZnO nanoparticles against pathogenic bacteria. *J Photochem Photobiol B.* 2015;146:52–57.
- Padalia H, Moteriya P, Chanda S. Synergistic antimicrobial and cytotoxic potential of zinc oxide nanoparticles synthesized using *Cassia auriculata* leaf extract. *Bionanoscience.* 2018;8(1):196–206.

27. Lowry J. *Trees for Wood and Animal Production in Northern Australia*. Indooroopilly, Queensland: Rural Industries Research and Development Corporation; 2008:89.
28. Lam SK, Ng TB, Sze Kwan L, Tzi Bun N. First report of an anti-tumor, anti-fungal, anti-yeast and anti-bacterial hemolysin from *Albizia lebbek* seeds. *Phytomedicine*. 2011;18(7):601–608.
29. Noté OP, Jihu D, Antheaume C, et al. Triterpenoid saponins from *Albizia lebbek* (L.) Benth and their inhibitory effect on the survival of high grade human brain tumor cells. *Carbohydr Res*. 2015;404:26–33.
30. Zare E, Pourseyedi S, Khatami M, Darezereshki E. Simple biosynthesis of zinc oxide nanoparticles using nature's source, and it's in vitro bio-activity. *J Mol Struct*. 2017;1146:96–103.
31. Bauer AW, Kirby WM, Sherris JC, Turck M. Antibiotic susceptibility testing by a standardized single disk method. *Am J Clin Pathol*. 1966; 45(4):493–496.
32. Pick E, Mizel D. Rapid microassays for the measurement of superoxide and hydrogen peroxide production by macrophages in culture using an automatic enzyme immunoassay reader. *J Immunol Methods*. 1981; 46(2):211–226.
33. Fraser SP, Ding Y, Liu A, Foster CS, Djamgoz MB. Tetrodotoxin suppresses morphological enhancement of the metastatic MAT-LyLu rat prostate cancer cell line. *Cell Tissue Res*. 1999;295(3):505–512.
34. Fraser SP, Diss JK, Chioni AM, et al. Voltage-gated sodium channel expression and potentiation of human breast cancer metastasis. *Clin Cancer Res*. 2005;11(15):5381–5389.
35. Kokila T, Ramesh PS, Geetha D. Biosynthesis of AgNPs using *Carica papaya* peel extract and evaluation of its antioxidant and antimicrobial activities. *Ecotoxicol Environ Saf*. 2016;134(Pt 2):467–473.
36. Nagarajan S, Arumugam Kuppusamy K. Extracellular synthesis of zinc oxide nanoparticle using seaweeds of gulf of Mannar, India. *J Nanobiotechnol*. 2013;11:39.
37. Singh BN, Rawat AK, Khan W, Naqvi AH, Singh BR. Biosynthesis of stable antioxidant ZnO nanoparticles by *Pseudomonas aeruginosa* rhamnolipids. *PLoS One*. 2014;9(9):e106937.
38. Anilreddy B. Preparation and characterization of iron oxide nanoparticles on disaccharide templates. *B JPRHC*. 2009;1(2):172–183.
39. Kumar B, Smita K, Cumbal L, Debut A. Synthesis of silver nanoparticles using Sacha inchi (*Plukenetia volubilis* L.) leaf extracts. *Saudi J Biol Sci*. 2014;21(6):605–609.
40. Kadam A, Dhabbe R, Gophane A, Sathe T, Garadkar K. Template free synthesis of ZnO/Ag₂O nanocomposites as a highly efficient visible active photocatalyst for detoxification of methyl orange. *J Photochem Photobiol B*. 2016;154:24–33.
41. Yuvakkumar R, Suresh J, Saravanakumar B, Joseph Nathanael A, Hong SI, Rajendran V. Rambutan peels promoted biomimetic synthesis of bioinspired zinc oxide nanochains for biomedical applications. *Spectrochim Acta A Mol Biomol Spectrosc*. 2015;137:250–258.
42. Raut S, Thorat PV, Thakare R. Green synthesis of zinc oxide (ZnO) nanoparticles using *Ocimum tenuiflorum* leaves. *Int J Sci Res*. 2013;4: 1225–1228.
43. Sinha R, Karan R, Sinha A, Khare SK. Interaction and nanotoxic effect of ZnO and Ag nanoparticles against ESBL and Amp-C producing gram negative isolates from superficial wound infections. *Int J Curr Microbiol Appl Sci*. 2015;1:38–47.
44. Gough DR, Cotter TG. Hydrogen peroxide: a Jekyll and Hyde signalling molecule. *Cell Death Dis*. 2011;2:e213.
45. Parashant GK, Prashant PA, Utpal B, et al. In vitro antibacterial and cytotoxicity studies of ZnO nanopowders prepared by combustion assisted facile green synthesis. *Karbala Int J Mod Sci*. 2015;1(2):67–77.
46. Bai Aswathanarayan J, Rai Vittal R, Muddegowda U, Jamuna BA, Ravishankar AV, Umashankar M. Anticancer activity of metal nanoparticles and their peptide conjugates against human colon adenorectal carcinoma cells. *Artif Cells Nanomed Biotechnol*. 2018; 46(7):1444–1451.
47. Mukherjee P, Bhattacharya R, Wang P, et al. Antiangiogenic properties of gold nanoparticles. *Clin Cancer Res*. 2005;11(9):3530–3534.
48. Fackler OT, Grosse R. Cell motility through plasma membrane blebbing. *J Cell Biol*. 2005;81:879–884.
49. Hanley C, Layne J, Punnoose A, et al. Preferential killing of cancer cells and activated human T cells using ZnO nanoparticles. *Nanotechnology*. 2008;19(29):295103.

International Journal of Nanomedicine

Publish your work in this journal

The International Journal of Nanomedicine is an international, peer-reviewed journal focusing on the application of nanotechnology in diagnostics, therapeutics, and drug delivery systems throughout the biomedical field. This journal is indexed on PubMed Central, MedLine, CAS, SciSearch®, Current Contents®/Clinical Medicine,

Submit your manuscript here: <http://www.dovepress.com/international-journal-of-nanomedicine-journal>

Dovepress

Journal Citation Reports/Science Edition, EMBase, Scopus and the Elsevier Bibliographic databases. The manuscript management system is completely online and includes a very quick and fair peer-review system, which is all easy to use. Visit <http://www.dovepress.com/testimonials.php> to read real quotes from published authors.